On the Construction of a High Order Difference Scheme for Complex Domains in a Cartesian Grid

E. Turkel and A. Yefet
School of Mathematical Sciences
Sackler Faculty of Exact Sciences
Tel Aviv University

Abstract

We consider fourth order accurate compact schemes for the numerical solutions of the two dimensional Maxwell equations. We base this scheme on Ty(2,4) scheme [4]. We solve the equations on a Cartesian mesh but consider boundaries which do not necessarily conform with the Cartesian grid. On the boundaries we use second or third order accurate approximations. We also discuss the numerical approximation to the PML layer.

1 Maxwell Equations

We consider the TM system and nondimensionalize the time. Let $\tau = ct = t/\sqrt{\mu\epsilon}$ and $Z = \sqrt{\frac{\mu}{\epsilon}}$ and set $Z = 1$. The TM wave equations then become:

$$\begin{aligned} \frac{\partial E_z}{\partial \tau} &= \frac{\partial H_y}{\partial x} - \frac{\partial H_x}{\partial y} \\ \frac{\partial H_x}{\partial \tau} &= -\frac{\partial E_z}{\partial y} \\ \frac{\partial H_y}{\partial \tau} &= \frac{\partial E_z}{\partial x}. \end{aligned} \tag{1}$$

2 Finite Differences Scheme

The Maxwell equations in one dimension are:

$$
\begin{aligned}
\frac{\partial E_z}{\partial \tau} &= \frac{\partial H_y}{\partial x} \\
\frac{\partial H_y}{\partial \tau} &= \frac{\partial E_z}{\partial x}
\end{aligned}
\tag{2}
$$

The grid is shown in Fig.1.

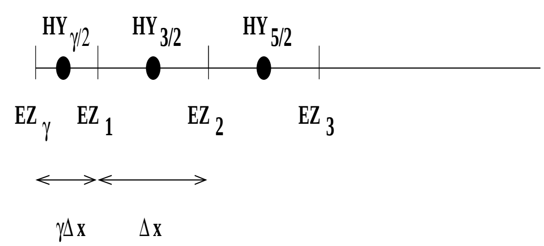

Figure 1: Location of the grid points

The interior scheme uses a compact implicit central difference formulation on a staggered mesh (see [4, 6]). This is the same placement of variables as in the Yee scheme. At the boundaries we need to alter the scheme since the boundary point need not coincide with a mesh node. We need to account for the nonuniform spacing near the boundaries. Therefore, at the boundaries instead of using $H_{Y\frac{1}{2}}$ we use $H_{Y\frac{\gamma}{2}}$ where $\gamma\Delta x$ is the distance between E_{Z1} and the first point $E_{Z\gamma}$. Define:

$$
\hat{M} = \begin{pmatrix}
a_l & 0 & . & . & . & . & 0 \\
a_{l1} & b_{l1} & c_{l1} & 0 & . & . & 0 \\
0 & 1 & 22 & 1 & 0 & . & 0 \\
. & . & . & . & & & \\
0 & . & 0 & 1 & 22 & 1 & 0 \\
0 & . & . & 0 & c_{r1} & b_{r1} & a_{r1} \\
0 & . & . & . & . & 0 & a_r
\end{pmatrix}, \quad
\hat{N} = \begin{pmatrix}
A_l & B_l & C_l & . & . & . & 0 \\
1 & 22 & 1 & 0 & . & . & 0 \\
0 & 1 & 22 & 1 & 0 & . & 0 \\
. & . & . & . & & & \\
0 & . & 0 & 1 & 22 & 1 & 0 \\
0 & . & . & 0 & 1 & 22 & 1 \\
0 & . & . & . & C_r & B_r & A_r
\end{pmatrix}.
$$

where:

$$
\begin{aligned}
a_l &= 24\gamma_l \\
a_{l1} &= \frac{8}{(1+\gamma_l)(3+\gamma_l)}, \quad b_{l1} = \frac{4(5+6\gamma_l)}{(1+\gamma_l)}, \quad c_{l1} = \frac{4}{(3+\gamma_l)} \\
A_l &= 3(3+4\gamma_l+\gamma_l^2), \quad B_l = 3(1-\gamma_l), \quad C_l = 0
\end{aligned}
$$

At the right boundary we use the same coefficients but with γ_r instead of γ_l.

We base these approximations on the following Taylor expansions:

$$\begin{aligned}
24\frac{E_{Z1}-E_{Z\gamma}}{\Delta x} &= a_l E_{Z\frac{\gamma}{2}x} + O(\Delta x^2) \\
24\frac{E_{Z2}-E_{Z1}}{\Delta x} &= a_{l1} E_{Z\frac{\gamma}{2}x} + b_{l1} E_{Z\frac{3}{2}x} + c_{l1} E_{Z\frac{5}{2}x} + O(\Delta x^3) \\
24\frac{H_{Y\frac{3}{2}}-H_{Y\frac{\gamma}{2}}}{\Delta x} &= A_l H_{Y1x} + B_l H_{Y2x} + C_l H_{Y3x} + O(\Delta x^2)
\end{aligned}$$

The matrix form of these approximations is:

$$\hat{M}\frac{\partial}{\partial x}\begin{bmatrix} E_Z^{\gamma_l/2} \\ E_Z^{3/2} \\ \cdot \\ \cdot \\ E_Z^{p-\gamma_r/2} \end{bmatrix} = \frac{24}{\Delta x}\begin{bmatrix} E_Z^1 - E_Z^{\gamma_l} \\ E_Z^2 - E_Z^1 \\ \cdot \\ E_Z^{p-1} - E_Z^{p-2} \\ E_Z^p - E_Z^{p-\gamma_r} \end{bmatrix}$$

$$\hat{N}\frac{\partial}{\partial x}\begin{bmatrix} H_Y^1 \\ H_Y^2 \\ \cdot \\ \cdot \\ H_Y^{p-1} \end{bmatrix} = \frac{24}{\Delta x}\begin{bmatrix} H_Y^{3/2} - H_Y^{\gamma_l/2} \\ H_Y^{5/2} - H_Y^{3/2} \\ \cdot \\ H_Y^{p-3/2} - H_Y^{p-5/2} \\ H_Y^{p-\gamma_r/2} - H_Y^{p-3/2} \end{bmatrix} .$$

If we have less than five mesh-grid points in any direction the treatment differs.

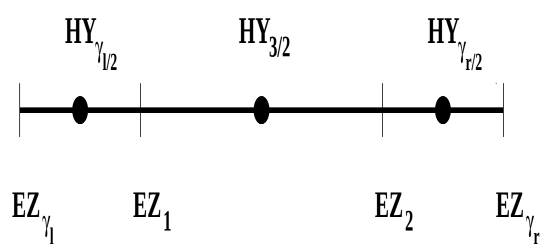

Figure 2: Location of the grid points

Suppose there are four mesh-grid points at the X direction (see fig 2), two of them are on the boundary. The relations are as follows:

$$\hat{M}\frac{\partial}{\partial x}\begin{bmatrix} E_Z^{\gamma_l/2} \\ E_Z^{3/2} \\ E_Z^{\gamma_r/2} \end{bmatrix} = \frac{24}{\Delta x}\begin{bmatrix} E_Z^1 - E_Z^{\gamma_l} \\ E_Z^2 - E_Z^1 \\ E_Z^{\gamma_r} - E_Z^2 \end{bmatrix}$$

$$\hat{N}\frac{\partial}{\partial x}\left[\begin{array}{c} H_Y^1 \\ H_Y^2 \end{array}\right] = \frac{24}{\Delta x}\left[\begin{array}{c} H_Y^{3/2} - H_Y^{\gamma_l/2} \\ H_Y^{\gamma_r/2} - H_Y^{3/2} \end{array}\right]$$

where

$$\hat{M} = \begin{pmatrix} 24\gamma_l & 0 & 0 \\ M_{21} & M_{22} & M_{23} \\ 0 & 0 & 24\gamma_r \end{pmatrix}, \quad \hat{N} = \begin{pmatrix} 3(3+4\gamma_l+\gamma_l^2) & 3(1-\gamma_l^2) \\ 3(1-\gamma_r^2) & 3(3+4\gamma_r+\gamma_r^2) \end{pmatrix}.$$

$$M_{21} = \frac{24}{3(1+\gamma_l)(2+\gamma_l+\gamma_r)}, \quad M_{22} = \frac{24(2+3\gamma_l+3\gamma_r+3\gamma_l\gamma_r)}{3(1+\gamma_l)(1+\gamma_r)}$$

$$M_{23} = \frac{24}{3(2+\gamma_l+3\gamma_r+\gamma_l\gamma_r+\gamma_r^2)}$$

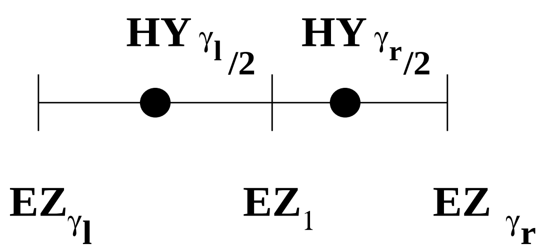

Figure 3: Location of the grid points

Now suppose there are three mesh-grid points in the X direction (fig 3), two of them are on the boundary. The relations are as follows:

$$\frac{2}{\gamma_l+\gamma_r}\frac{H_{Y\,\gamma_r/2} - H_{Y\,\gamma_l/2}}{h} = H_{Y\,1x}$$

$$\frac{E_{Z\,1} - E_{Z\,\gamma_l}}{\gamma_l h} = E_{Z\,\gamma_l/2x}$$

$$\frac{E_{Z\,\gamma_r} - E_{Z\,1}}{\gamma_r h} = E_{Z\,\gamma_r/2x}$$

We shall refer to this scheme with the various boundary possibilities as comTy(2,4).

3 Numerical Treatment of the PML

In order to absorb waves at the outer boundary we shall use a PML layer [1, 5]. These layers all have lower order terms which can cause numerical instabilities. To describe what happens we first discuss a one dimensional scalar equation.

$$u_t + f_x + \sigma u = 0 \tag{3}$$

where σ is a constant and f some general flux. To increase the stability of the method we introduce exponential differencing. We find that this delays long term instabilities compares to an explicit or implicit treatment of the lower order terms. Hence, we introduce $v = e^{\sigma t}u$. Then (3) becomes

$$e^{-\sigma t}v_t + f_x = 0 \tag{4}$$

We shall use a leapfrog method in time and some general differencing Df to approximate f_x. The approximation to (4) becomes

$$e^{-\sigma(n+\frac{1}{2})\Delta t}\ \frac{v_j^{n+1} - v_j^n}{\Delta t} + Df_j^{n+\frac{1}{2}} = 0. \tag{5}$$

Rewriting (5) in terms of u we get

$$\frac{u_j^{n+1}e^{\frac{\sigma\Delta t}{2}} - u_j^n e^{-\frac{\sigma\Delta t}{2}}}{\Delta t} + Df_j^{n+\frac{1}{2}} = 0 \tag{6}$$

We next consider a gneralization of the Berenger PML that is presented in [5], eq. (5.4). For the two dimensional TM equations the PML becomes

$$\begin{aligned}
\frac{\partial E_z}{\partial t} + (\sigma_x + \sigma_y)E_z + \sigma_x\sigma_y P_z &= \frac{\partial H_y}{\partial x} - \frac{\partial H_x}{\partial y} \\
\frac{\partial H_x}{\partial t} + (\sigma_y - \sigma_x)H_x + \sigma_x(\sigma_x - \sigma_y)Q_x &= -\frac{\partial E_z}{\partial y} \\
\frac{\partial H_y}{\partial t} + (\sigma_x - \sigma_y)H_y + \sigma_y(\sigma_y - \sigma_x)Q_y &= \frac{\partial E_z}{\partial x} \\
\frac{\partial P_z}{\partial t} &= E_z \\
\frac{\partial Q_x}{\partial t} &= H_x - \sigma_x Q_x \\
\frac{\partial Q_y}{\partial t} &= H_y - \sigma_y Q_y
\end{aligned} \tag{7}$$

$\sigma_x = \sigma_x(x)$, $\sigma_y = \sigma_y(y)$. When there is a PML layer in only the x direction then $\sigma_y = 0$ and the only artificial variable needed is Q_x. All three artificial variables are needed only in corner regions. Differencing (7) based on the model of (6) we have

$$
\begin{aligned}
\frac{e^{\frac{(\sigma_x+\sigma_y)\Delta t}{2}} E_z^{n+1} - e^{-\frac{(\sigma_x+\sigma_y)\Delta t}{2}} E_z^n}{\Delta t} + \sigma_x \sigma_y P_z^{n+\frac{1}{2}} &= \left(\frac{\partial H_y}{\partial x} - \frac{\partial H_x}{\partial y} \right)^{n+\frac{1}{2}} \\
\frac{e^{\frac{(\sigma_y-\sigma_x)\Delta t}{2}} H_x^{n+\frac{1}{2}} - e^{-\frac{(\sigma_y-\sigma_x)\Delta t}{2}} H_x^{n-\frac{1}{2}}}{\Delta t} + \sigma_x(\sigma_x - \sigma_y) Q_x^n &= -\frac{\partial E_z^n}{\partial y} \\
\frac{e^{\frac{(\sigma_x-\sigma_y)\Delta t}{2}} H_y^{n+\frac{1}{2}} - e^{-\frac{(\sigma_x-\sigma_y)\Delta t}{2}} H_y^{n-\frac{1}{2}}}{\Delta t} + \sigma_y(\sigma_y - \sigma_x) Q_x^n &= \frac{\partial {E_z}^n}{\partial x} \\
\frac{P_z^{n+\frac{1}{2}} - P_z^{n-\frac{1}{2}}}{\Delta t} &= E_z^n \\
\frac{e^{\frac{\sigma_x \Delta t}{2}} Q_x^{n+1} - e^{\frac{-\sigma_x \Delta t}{2}} Q_x^n}{\Delta t} &= H_x^{n+\frac{1}{2}} \\
\frac{e^{\frac{\sigma_y \Delta t}{2}} Q_y^{n+1} - e^{\frac{-\sigma_y \Delta t}{2}} Q_y^n}{\Delta t} &= H_y^{n+\frac{1}{2}}
\end{aligned}
\tag{8}
$$

4 Computational-Results

We test this scheme on a circular perfect conductor. The exact solution in this case is:

$$
\begin{aligned}
E_Z &= J_1(\omega r)\sin(\theta + \omega t) \\
H_Y &= -\frac{x}{r}\left[\frac{J_0(\omega r) - J_2(\omega r)}{2}\right]\cos(\theta + \omega t) \\
&\quad - \frac{y J_1(\omega r)\sin(\theta + \omega t)}{\omega r^2} \\
H_X &= \frac{y}{r}\left[\frac{J_0(\omega r) - J_2(\omega r)}{2}\right]\cos(\theta + \omega t) \\
&\quad - \frac{x J_1(\omega r)\sin(\theta + \omega t)}{\omega r^2}
\end{aligned}
$$

where $r = \sqrt{x^2 + y^2}$ and $\theta = \arctan(y/x)$.

Setting $E_Z = 0$ on $r = 1/2$ requires that $\omega = 14.03117333963124$. For the initial values we choose:

$$
\begin{aligned}
E_Z &= J_1(\omega r)\sin(\theta) \\
H_Y &= -\frac{x}{r}\left[\frac{J_0(\omega r) - J_2(\omega r)}{2}\right]\cos(\theta + \frac{\omega \Delta t}{2}) \\
&\quad - \frac{y J_1(\omega r)\sin(\theta + \frac{\omega\Delta t}{2})}{\omega r^2} \\
H_X &= \frac{y}{r}\left[\frac{J_0(\omega r) - J_2(\omega r)}{2}\right]\cos(\theta + \frac{\omega \Delta t}{2}) \\
&\quad - \frac{x J_1(\omega r)\sin(\theta + \frac{\omega\Delta t}{2})}{\omega r^2}
\end{aligned}
$$

We advance in time using the leapfrog scheme. We tested this scheme for three sets of grids. In the first case $\Delta x = \Delta y = \frac{1}{20}$, $\Delta t = 1/360$, in the second case $\Delta x = \Delta y = \frac{1}{40}$, $\Delta t = 1/720$ and for the third case we choose $\Delta x = \Delta y = \frac{1}{80}$, $\Delta t = 1/1440$. In figure 4 we display the errors as a function of time while in figure 5 we display the errors as a function of the mesh size.

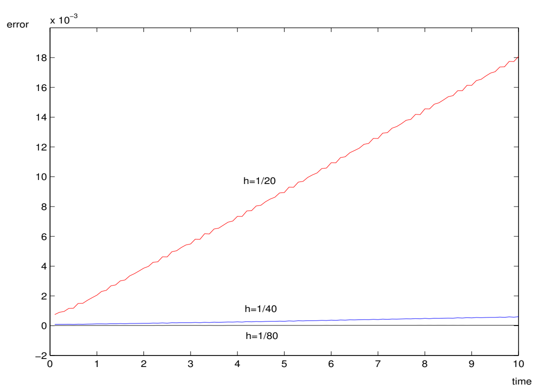

Figure 4: The errors between the exact solution and the approximation in L_2 norm.

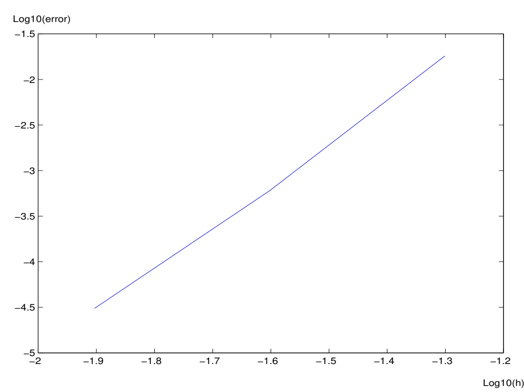

Figure 5: Log_{10}(error) as a function of $Log_{10}(h)$ at $t = 10$.

We next compare the comTy(2,4) scheme with staircasing. Due to the artificial corners introduced by staircasing the Ty(2,4) scheme is only first order accurate. In Fig(6a)-(6c) we display the errors in the L_2 norm for both schemes, the staircased Ty(2,4) and the comTy(2,4) schemes. The errors in the staircased Ty(2,4) are quasi-periodic in time. When the mesh is refined the periods increase.

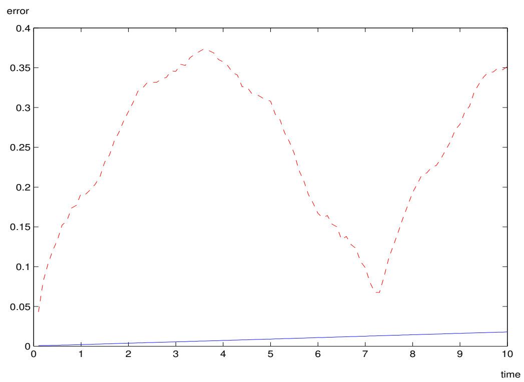

Figure 6a: The errors, in L_2 norm. The staircased Ty(2,4) is drawn by dashed lines and the comTy(2,4) is drawn by solid line. $h = 1/20$ and $\Delta t = 1/360$

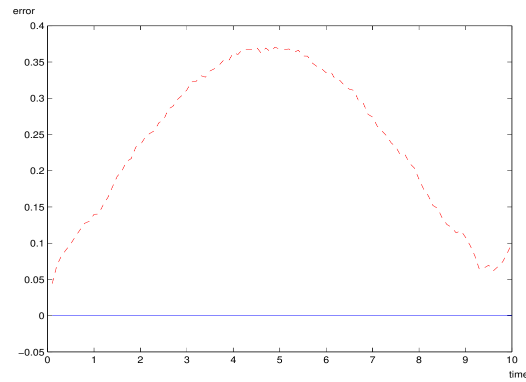

Figure 6b: Same as 6a but with $h = 1/40$ and $\Delta t = 1/720$

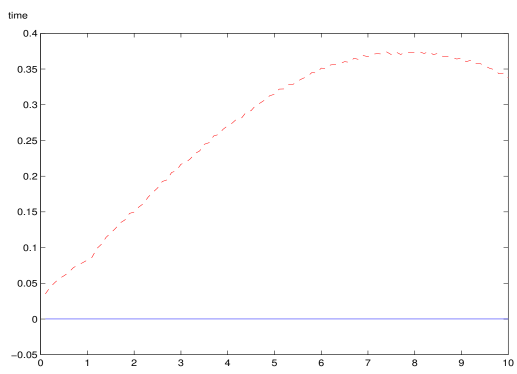

Figure 6c: Same as 6a but with $h = 1/80$ and $\Delta t = 1/1440$

In table 1 we present the errors in the L_2 norm for the staircased Ty(2,4) and the comTy(2,4) schemes. In both cases the error is linear in time. However, as the mesh is refined the staircasing technique yields first order accuracy while the comTy(2,4) yields between fourth and fifth order accuracy. In all cases the comTy(2,4) scheme is considerably more accurate than the staircased Ty(2,4) scheme.

scheme	h	Δt	$t=1$	t=10
$Ty(2,4)$	$\frac{1}{20}$	$\frac{1}{360}$	0.0021	0.0181
$comTy(2,4)$	$\frac{1}{40}$	$\frac{1}{720}$	1.230×10^{-4}	6.02×10^{-4}
$comTy(2,4)$	$\frac{1}{80}$	$\frac{1}{1440}$	1.764×10^{-5}	3.0824×10^{-5}
staircase	$\frac{1}{20}$	$\frac{1}{360}$	0.1923	0.3514
staircase	$\frac{1}{40}$	$\frac{1}{720}$	0.1399	0.0999
staircase	$\frac{1}{80}$	$\frac{1}{1440}$	0.0826	0.3379

Table 1: Errors in L_2 norm for various times

Next we consider a computational domain which is bounded by the curves $Y = \tan(\frac{3\pi}{7})X$, $X^2+Y^2 = \frac{1}{4}$ and the X-axis (see figure 7). We assume that the the boundaries of the sector are perfect conductors.

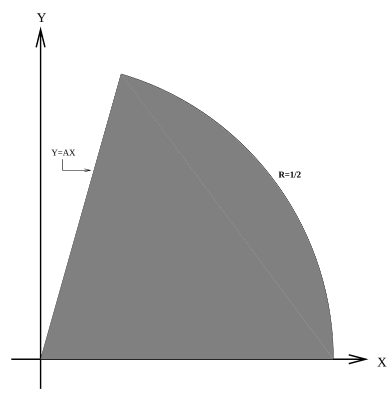

Figure 7: The computational domain.

The exact solution in this case is

$$
\begin{aligned}
E_Z &= J_\nu(\omega r)\sin(\nu\phi)\cos(\omega t) \\
H_Y &= \frac{x}{2r}\left[J_{\nu-1}(\omega r) - J_{\nu+1}(\omega r)\right]\sin(\nu\phi)\sin(\omega t) \\
&\quad - \frac{\nu y}{\omega r^2} J_\nu \cos(\nu\phi)\sin(\omega t) \\
H_X &= -\frac{y}{2r}\left[J_{\nu-1}(\omega r) - J_{\nu+1}(\omega r)\right]\sin(\nu\phi)\sin(\omega t) \\
&\quad - \frac{\nu x}{\omega r^2} J_\nu(\omega r)\cos(\nu\phi)\sin(\omega t)
\end{aligned}
$$

where

$$\omega = 16.75883874736728 \qquad \nu = \frac{14}{3}$$
$$r = \sqrt{x^2 + y^2} \qquad \phi = \arctan(\frac{y}{x})$$

Setting $E_Z = 0$ on the boundary requires that $\omega = 16.75883874736728$ and $\nu = \frac{14}{3}$. We test the new scheme for three levels of grid refinement. In the first case $\Delta x = \Delta y = \frac{1}{20}$, $\Delta t = 1/360$, for the second case $\Delta x = \Delta y = \frac{1}{40}$, $\Delta t = 1/720$ and for the third case $\Delta x = \Delta y = \frac{1}{80}$, $\Delta t = 1/1440$. In figure 8 the errors as a function of time are displayed while in figure 9 we draw the errors as a function of the mesh spacing.

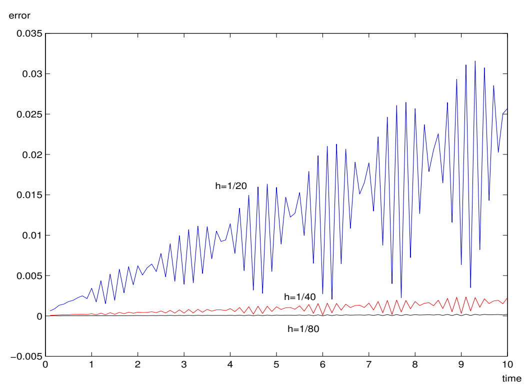

Figure 8: The errors in L_2 norm.

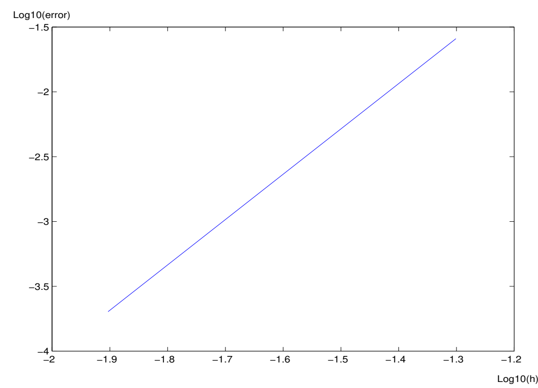

Figure 9: $Log_{10}(error)$ as a function of $Log_{10}(h)$ at $t = 10$.

We compare the comTy(2,4) scheme with the staircased Ty(2,4). In Fig(10a)-(10c) we show the errors in L_2 norm for both schemes, the staircased Ty(2,4) and the comTy(2,4) schemes. One observes that the staircased Ty(2,4) is first order accurate. The comTy(2,4) yields between third and fourth order accuracy and is considerably more accurate than the staircased Ty(2,4).

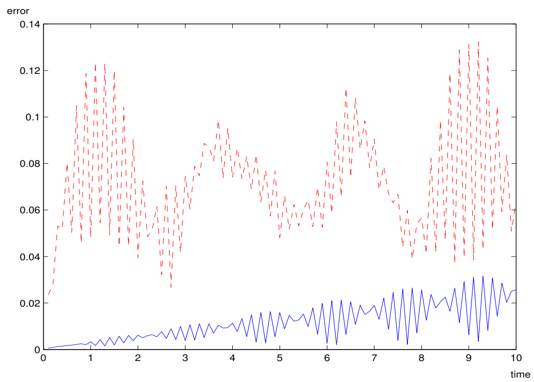

Figure 10a: Errors in L_2 norm. The staircased Ty(2,4) drawn by dashed lines and comTy(2,4) by solid line $h = 1/20, \Delta t = 1/360$.

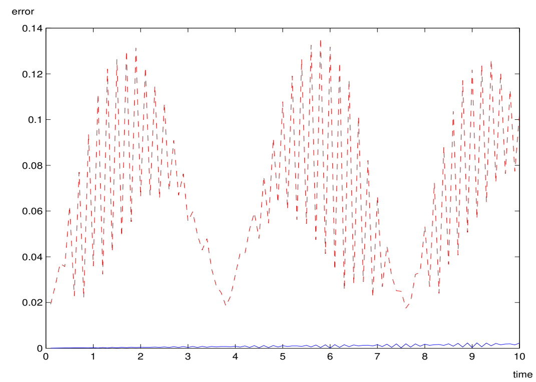

Figure 10b: Same as 10a with $h = 1/40$ and $\Delta t = 1/720$

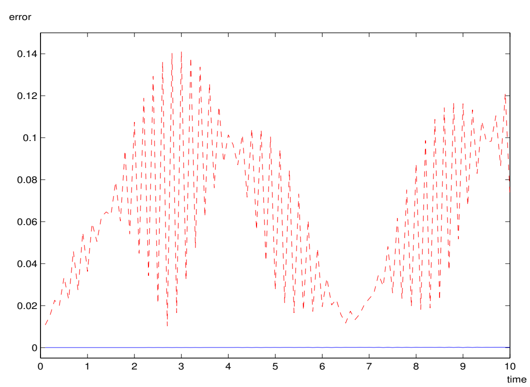

Figure 10c: Same as 10a with $h = 1/80$ and $\Delta t = 1/1440$

In table 2 we present the errors, in the L_2 norm, for the staircased Ty(2,4) and the comTy(2,4) schemes. In both cases the error are linear in time. The staircasing technique yields first order accuracy while the comTy(2,4) yields between third and fourth order accuracy. In all cases the comTy(2,4) scheme is considerably more accurate than the staircased Ty(2,4) scheme.

$scheme$	h	Δt	$t=1$	t=10
$comTy(2,4)$	$\frac{1}{20}$	$\frac{1}{360}$	0.0034	0.0257
$comTy(2,4)$	$\frac{1}{40}$	$\frac{1}{720}$	2.8×10^{-4}	0.0023
$comTy(2,4)$	$\frac{1}{80}$	$\frac{1}{1440}$	2.6×10^{-5}	2.0×10^{-4}
$staircase$	$\frac{1}{20}$	$\frac{1}{360}$	0.0481	0.0640
$staircase$	$\frac{1}{40}$	$\frac{1}{720}$	0.0360	0.1030
$staircase$	$\frac{1}{80}$	$\frac{1}{1440}$	0.0364	0.0720

Table 2: Errors in L_2 norm for various times.

References

[1] J-P Berenger, "A Perfectly Matched Layer for the Absorption of Electromagnetic Waves," *Journal of Computational Physics*, Vol. 114, pp 185-200, 1994.

[2] S. Gedney, *The Perfectly Matched Layer Absorbing Medium* in **Advances in Computational Electrodynamics: The Finite-Difference Time-Domain Method**, A. Taflove, editor, Artech House, 263-343, 1998.

[3] R.F. Harrington, *Time-Harmonic Electromagnetic Fields,* Magraw-Hill, 1961.

[4] E. Turkel and A. Yefet, *Fourth Order Accurate Compact Implicit Method for the Maxwell Equations*, to appear.

[5] E. Turkel, A. Yefet *Absorbing PML Boundary Layers for Wave-Like Equations*, Applied Numerical Mathematics, 27:533-557, 1998.

[6] E. Turkel, *High Order Methods* in **Advances in Computational Electrodynamics: The Finite-Difference Time-Domain Method**, A. Taflove, editor, Artech House, 63-109, 1998.